

Photo-triggered pulsed cavity compressor for bright electron bunches in ultrafast electron diffraction

G. H. Kassier · N. Erasmus · K. Haupt ·
I. Boshoff · R. Siegmund · S. M. M. Coelho ·
H. Schwoerer

Received: 16 April 2012/Revised: 20 July 2012/Published online: 27 September 2012
© Springer-Verlag 2012

Abstract Temporally resolved observation of microscopic structural dynamics of solids with ultrafast electron diffraction (UED) requires extremely short pulsed, highly charged, monoenergetic electron beams with sufficient transverse coherence length of several unit cells of the investigated samples. However, Coulomb repulsion defeats these parameters in free propagation of an electron pulse initially bright on the photo cathode. We demonstrate a new electron pulse compressor design based on a simple

and compact RF structure incorporating a pair of gallium arsenide photoconductive semiconductor switches that are triggered by femtosecond laser pulses, thereby providing a longitudinal voltage gradient of up to 20 V/ps. Our proof of principle experiment achieved compression of bunches containing 26,000 electrons to a duration of below 750 fs and a beam diameter of 300 μm in the temporal and spatial focus of the device while maintaining the good beam collimation required for time resolved electron diffraction experiments. The simplicity of the compressor provides a strong incentive for its further development toward practical implementation in sub-relativistic UED experiments requiring the highest possible source brightness.

G. H. Kassier · N. Erasmus · K. Haupt · I. Boshoff ·
R. Siegmund · H. Schwoerer
Physics Department, Laser Research Institute,
Stellenbosch University, Stellenbosch, South Africa
e-mail: nerasmus@sun.ac.za

K. Haupt
e-mail: haupt@sun.ac.za

I. Boshoff
e-mail: iboshoff@sun.ac.za

R. Siegmund
e-mail: rene.siegmund85@googlemail.com

H. Schwoerer
e-mail: heso@sun.ac.za

G. H. Kassier
Max Planck Research Department, Centre for Free Electron
Laser Science, University of Hamburg, Hamburg, Germany

Present Address:

G. H. Kassier (✉)
c/o DESY, Notke Strasse 85, Building 222,
room 110, 22607 Hamburg, Germany
e-mail: gunther.kassier@mpsdlcfel.de

S. M. M. Coelho
Department of Physics, University of Pretoria,
Pretoria 0002, South Africa
e-mail: sergio.coelho@up.ac.za

1 Introduction

The investigation of structural dynamics and collective electron dynamics in solids with both atomic spatial and temporal resolution is instigated by the enormous progress in the development of femtosecond X-ray and electron sources for time resolved diffraction experiments within the last decade. In particular, photo-induced microscopic dynamics in strongly correlated electronic systems and inorganic crystals are now accessible through real time observation of electron–phonon coupling, charge density wave dynamics and proton transfer reactions [1–3].

Synchrotron and free electron laser-based X-ray sources, table top laser-driven X-ray sources and compact femtosecond electron guns compete and complement each other with their respective strengths and limitations. Temporal resolution in all devices is achieved using femtosecond laser pulses as the initial source and a pump-probe type arrangement for the experimental procedure; spatial resolution is obtained using the X-ray or deBroglie wavelength, respectively.

Notable achievements in ultrafast X-ray diffraction (XRD) science and technology have been made in the last decade. Plasmas produced by intense femtosecond laser pulses on metal surfaces can produce ultrashort pulses of narrowband hard X-rays due to inner shell ionization by laser accelerated electrons and subsequent immediate line emission. Such sources have been applied to the study of fs laser-produced shock waves and phonons in simple crystalline targets [4, 5], and recently in a powder diffraction geometry in an ionic crystal [3]. Efficiencies have been improved and laser requirements have been relaxed in the last decade [6, 7], thus compensating for the low scattering cross section of X-rays in matter, while retaining a reasonably compact experimental system.

Ultrafast electron diffraction (UED) is an attractive and compact alternative to ultrafast XRD. Electrons have the advantage of up to 10^6 times higher scattering cross section compared with X-rays. In addition, electron optics are considerably simpler and more efficient than their X-ray counterparts. However, the electric charge responsible for the excellent scattering cross section of electrons leads to rapid de-bunching of bright femtosecond electron pulses in all directions, thereby spoiling the temporal resolution potential. For example, according to ASTRA [8] simulations, we find that an initially 200 fs short electron pulse with 50 μm diameter comprising of 100,000 electrons, accelerated to 30 keV within 4 mm, will be 10 ps long after 15 cm of propagation. Therefore, subrelativistic UED sources of the first generation have to be compact and operate with very low electron numbers per pulse. Most notably, Siwick et al. [9] achieved pulses containing about 10^4 electrons with a duration of about 550 fs using a very compact 55 kV direct current (DC) photogun, as measured by Hebeisen et al. [10]. Pulses produced by this device have appropriate coherence properties for time resolved investigation of photo-induced structural and electronic phase transitions in metals and crystals, see for example [1, 11–13].

In order to extend UED experiments to the fastest possible structural dynamics processes as well as to more complicated crystal structures, or to samples that cannot be repeatedly excited and probed, the achievement of very bright sub-100 fs electron bunches containing in the order of 10^6 electrons is imperative. These pulses would allow recording of a diffraction pattern in a single or very few shots. Space charge-induced de-bunching precludes existing sub-relativistic DC photoguns from achieving such a high brilliance. Accelerating electrons to relativistic energies, where the temporal dispersion rate is strongly damped can be a solution [14]. Yet MeV electron accelerator technology is bulky, expensive, and unlikely to allow for a true table-top setup.

The alternative is to re-compress the expanding electron bunches emanating from DC photoguns. In the presence of

space charge forces, electron pulses emanating from photoguns inherently possess a chirp that leads to de-bunching. Electron bunch compression can be effected by imparting a linear position-momentum correlation (chirp) on an electron pulse such that trailing electrons in the bunch have a larger momentum than the ones at the front by a suitable beam line element. Such a linear chirp results in bunch compression at a certain position along the beam trajectory. Optimal compression is possible, provided that the imparted compressive chirp is large enough, and that the space charge forces, and consequently the electron momentum, are linear functions of the longitudinal electron position in the bunch [15]. This is the case for hard edged, uniformly populated ellipsoidal bunches, which have been shown to arise quite naturally from femtosecond electron pulses emitted from standard photocathodes as used in UED [16]. While ideal ellipsoidal electron bunches will, strictly speaking, only evolve if the initial radial electron distribution at the photocathode has a “half circle” profile, reasonably good results do not depend sensitively on this such that more easily attainable Gaussian or truncated Gaussian profiles are also satisfactory.

Conventional radio frequency (RF) accelerator technology is perhaps the most obvious choice for practical electron bunch re-compression. While Fill et al. [17] numerically considered a pillbox cavity for electron bunch compression in UED, the first practical compressing UED source concept was based on a high quality factor (Q) cavity to be driven by a solid state RF amplifier [16]. Successful realisation of this concept ensued quite recently [18]. Technical challenges associated with this concept are the high machining tolerances necessary for the RF cavity, as well as the need for sophisticated electronics for precise synchronization of the electron pulse and the RF amplifier.

Instead of actively imparting a linear chirp to electron bunches, it is possible to passively invert the existing (linear) chirp for compression of the bunch. One example of this approach is an achromatic reflectron compressor proposed by some of us [19]. While it has the allure of requiring only static beamline elements, the reflectron does not allow for active control of the electron energy bandwidth; it merely reverses the existing chirp of electron pulses without increasing (or decreasing) the total energy spread. Since the latter, together with the time-bandwidth product of the electron bunches, determines the pulse duration at the temporal focus, reflectron compressors ultimately cannot match the achievable electron density and pulse duration of their RF counterparts. Nonetheless, the appeal of the inherently jitter-free nature of reflectron compression suggests that this concept may yet play a significant role in UED, particularly for higher electron energies in the few 100 keV range where RF compressors would become very bulky and expensive. Recent publication of an alternative achromatic reflectron design indicates that

the UED community is showing some interest in this concept [20]. The compactness of the original achromatic reflectron [19], so chosen as to minimise the pulse duration at the temporal focus subject to spatial constraints as determined by the electron gun and other beamline elements, is absent in this design.

Another compressor design based on conventional magnetic chicanes was proposed for relativistic laser plasma accelerated electron bunches [21]. The compressor is applied to electrons accelerated by a strong laser field within a solid state density plasma. The inherent instability of this laser acceleration concept, for example compared to self modulated wake field acceleration in gas targets [22], complicates application of the scheme in sensitive time-resolved electron diffraction experiments on complex samples.

In this article, we present the realisation of a novel compact electron bunch compressor based on a special RF oscillator [23]. Unlike conventional RF compressors which utilise high Q closed cavities that are resonantly driven by remote amplifiers, we employ an open resonant structure that already incorporates the active electronics required for phase-stable high power RF oscillation in a simple and elegant way. The need for high Q is avoided by utilising only the first half period of a laser-triggered damped oscillation as a compression cycle for injected sub-relativistic electron pulses emanating from a fs laser triggered DC photogun. In combination with a magnetic solenoid lens pair as used in previous RF compressor UED setups [16, 18], our first implementation allows for compression of a 20 kV electron bunch with 26,000 electrons to less than 750 fs and a spot diameter of 300 μm at the temporal focus. Relaxation of the tight spatial focus at the point of maximal pulse compression along with some reduction of the electron number has yielded 200 fs pulse durations, thereby establishing the low jitter nature of our device. Due

to direct optical locking of the electron source, compressor and target pumping, the system has an excellent long-term temporal stability of sub 200 fs over 24 h, which stimulates further development of this concept towards extremely bright UED compressor guns.

2 Experimental

The compressor is part of an UED setup, headed by an amplified femtosecond laser (ClarkMXR CPA2101) delivering 150 fs long pulses at a wavelength of 775 nm with a repetition rate of 1,000 Hz and an average power output of about 0.7 W. A fraction of the pulse energy is diverted by a beamsplitter and frequency tripled ($\lambda = 258$ nm, $E = 4.8$ eV). The resulting UV pulses are focused to a spot diameter of 30 μm on a 10 nm thin film gold on sapphire photocathode [24] inside a vacuum chamber, on which they generate an ultrashort bunch of photoelectrons. The cathode potential is variable in the 10–45 kV range. The grounded anode with a 2 mm central hole is placed at a distance of 4 mm from the cathode to ensure rapid acceleration. The first of two magnetic lenses, placed 30 mm from the cathode, collimates the electron beam (see also Fig. 1).

The electron pulse compressor is placed 160 mm downstream of the photo cathode. It consists of two circular electrodes (diameter 7.5 mm, distance 2.5 mm) with central holes of 2 mm diameter, spaced by two gallium arsenide (GaAs) wafers, acting as photoconductive semiconductor switches (PCSS) (see Fig. 2). The GaAs PCSS were fabricated by evaporating straight edged ohmic contacts onto 4×6 mm² sized, 0.5 mm thick GaAs wafers with a dark resistivity of about 10^6 Ω cm. The metallisation consisted of titanium (5 nm)/germanium-gold (200 nm)/gold (200 nm) deposited by thermal evaporation and subsequent annealing

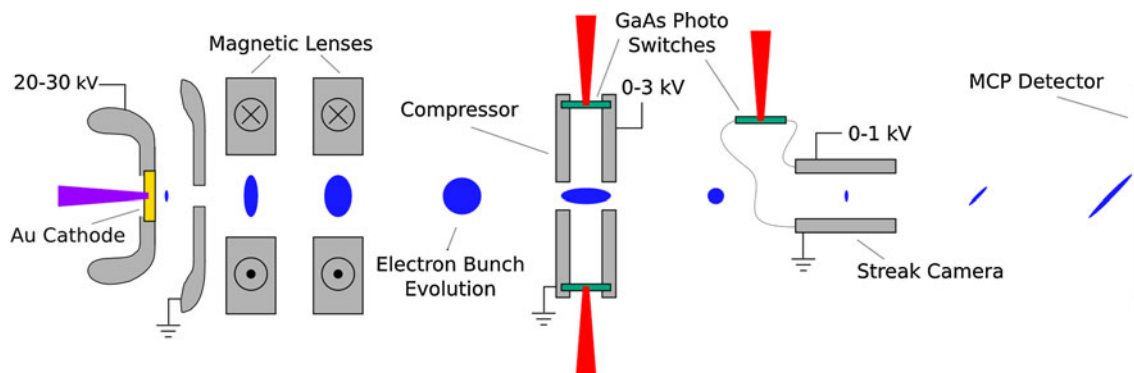


Fig. 1 Schematic diagram of the compressor setup. Short electron pulses are generated by 256 nm UV pulses (duration <150 fs) at the thin film gold photocathode, and accelerated to 20 kV over a short distance of 4 mm. Space charge and radial electric fields at the anode extraction aperture lead to radial beam expansion, which is reversed by a pair of solenoid magnetic lenses. Space charge forces result in

temporal expansion of the electron pulses to the picosecond time domain at the position of the photo triggered pulse compressor, which reverses this expansion for suitable laser trigger timing. The self-compressing pulses are measured at the point of minimal pulse duration using a photo-triggered streak camera

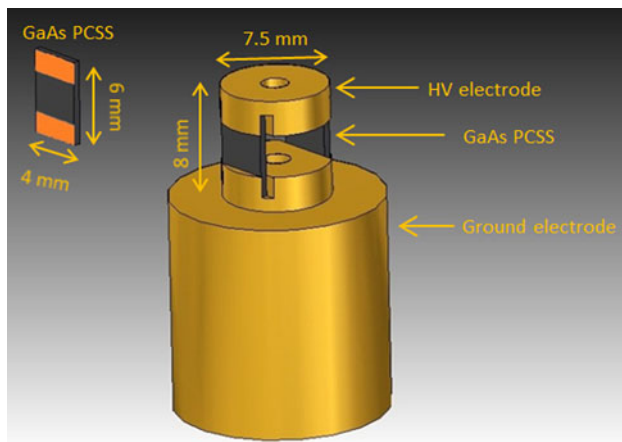


Fig. 2 Geometry of the pulsed compressor. The assembly consists of a high voltage (HV) electrode shunted to a ground electrode by a pair of GaAs PCSS's. An instance of the latter is also shown removed from the assembly on the left side of the sketch, and here the switch metallisation is visible. The trigger laser pulses impinge on the outward facing sides of the GaAs PCSS's, the electron pulses pass through the 2 mm holes in the electrodes in an upward direction. The high voltage (HV) pulser is connected to the HV electrode via the charging resistors (not shown in the figure)

at 450 °C for 2 min in an argon-filled furnace. The switch gap between the electrodes measured roughly 2.5 mm (see Fig. 2). The HV electrode is charged up to 2.6 kV by a pulser for a time window of about 50 ns around the electron pulse arrival time at the compressor. The in house built pulser employs a Behlke HTS 121 switch in addition to a critically damped LCR circuit so that the 50 ns pulse width can be achieved. These short electric charging pulses are thought to prevent avalanche breakdown (also known as the lock on effect) in the GaAs PCSS's that would lead to failure already at a few hundred volts DC. In addition, we believe that the danger of surface flashover at the GaAs–vacuum interface due to secondary electron-induced charging effects is minimised when sub-100 ns pulses are applied. Despite these measures for maximising the voltage that can be switched by the GaAs PCSS's, we have found that the devices presently used are not capable of switching voltages larger than about 3 kV, while switch holdoff voltages of up to 5 kV were observed without laser triggering. Failure is believed to result from damage due to surface current heating effects that form conductive pathways on the GaAs surface beginning at and progressing from the edge of the switch metallisation. We have also considered surface tracking due to secondary electrons as a failure mechanism, but rejected this hypothesis based on the fact that switch failure voltages did not improve when the switches were placed in a protective dielectric medium (transformer oil, deionised water and a transparent varnish coating were all tested as protective dielectrics).

The GaAs PCSS's are synchronously pumped by two laser pulses (wavelength 775 nm, duration 150 fs, pulse energy

60 μJ , intensity approximately 10^{10} W/cm^2). The symmetric assembly of the switches ensures a spatially homogeneous electric field gradient dE/dt during the discharge. Due to a charging resistor coupled in series with the compressor, it is initially decoupled from the HV supply, and the electrode discharges in a damped oscillation. A second magnetic lens centered 80 mm in front of the compressor compensates additional beam divergence introduced by the compressor's defocusing electric field and space charge, thus ensuring a small and well-collimated electron beam on target.

The oscillation frequency of the compressor is mainly determined by the device geometry and dielectric properties of the GaAs PCSS's. It was measured to be 4.5 GHz by recording the electron pulse arrival time as a function of cavity oscillation phase using a low-jitter high resolution streak camera [25]. The streak camera was placed 80 mm downstream of the compressor at the position of the envisaged temporal focus, and in addition to compressor frequency and phase determinations, it was used to determine the temporal duration of the electron pulses. The streak camera relies on the same photo triggered PCSS concept as the compressor, and is demonstrably capable of 150 fs temporal resolution [25]. Electrons are detected with a micro-channel plate coupled to a fluorescence screen and a Peltier cooled CCD camera. The electron number per bunch was measured using a Faraday cup coupled to a picoammeter.

The optimal cavity phase for successful compression occurs if the electron bunch centre passes the compressor centre at the instant when the compressor electric field changes sign for the first time. At this point, the temporal electric field gradient is linear for about 30 ps (approximately 1/8 of an oscillation), and amounts to about $dE/dt = 100$ $\text{V}/(\text{cm ps})$. It causes a delay of electrons ahead of the bunch centre, and advancement of trailing electrons. Furthermore, the bunch centre arrival time at the envisaged temporal focus remains unaltered by the compressor so as to minimise timing jitter arising from compressor charging voltage variations. Experimentally, this optimum compressor phase is easily determined by adjusting the compressor laser trigger delay stage until the first negative compressor delay versus streak camera arrival time trend is observed. Fine-tuning of the compressor delay until there is a zero net deflection of the observed streak image centre relative to the unstreaked position optimises the compressor phase.

The design of the compressor beamline, from the photogun through the two magnetic lenses and the compressor to the temporal focus position, was aided by many-body charged-particle propagation simulations. The electric and magnetic fields of the beamline elements were computed from the relevant geometries using the Poisson Superfish set of codes [26]. For the compressor, a simplified geometry that neglects the presence of the GaAs PCSS's was used to calculate the electrostatic field, see Fig. 3. Harmonic

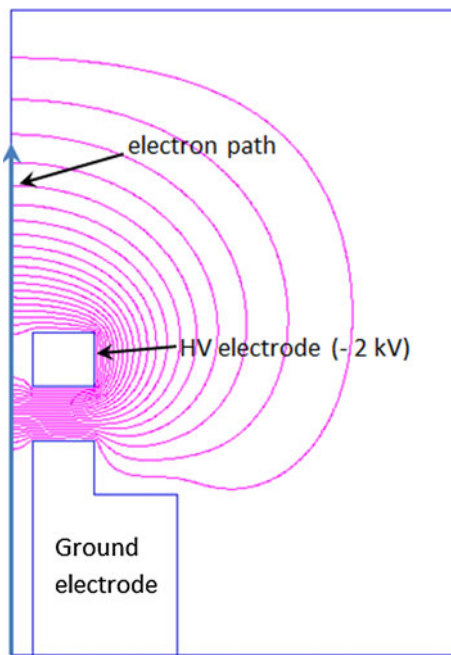


Fig. 3 Electric potential distribution for a simplified version of the compressor for the case of a static 2 kV potential applied at the HV electrode. Full radial symmetry was assumed, and the presence of the GaAs photoswitches was ignored in this Poisson Superfish [26] simulation. The effect of the cavity on the electron pulses was modelled by harmonic modulation of the computed on axis static electric field profile

modulation of this spatial electric field in time with a frequency of 4.5 GHz yielded an approximation of the effect of the cavity on the electron bunch tracking simulations. The latter were accomplished with the ASTRA code [8]. The simulated performance of the setup shown in Fig. 1, subject to optimised lens currents and an assumed peak compressor voltage of 2.5 kV, is given in Fig. 4.

The main optimisation criterion was achievement of a well-collimated electron beam of small size ($<300\ \mu\text{m}$ diameter) at the position of the temporal focus. Obviously, a short temporal duration of order 100 fs is desired, and according to Fig. 4, these simultaneous goals are realistic. The lens current values and compressor voltage suggested by the simulations were applied as starting values in the experimental setup, and adjusted until a desired beam diameter of $<300\ \mu\text{m}$, good collimation and maximal compression were achieved.

In order to test the theoretical limits of this compressor in terms of electron number per pulse while retaining femtosecond pulse duration, further simulations were carried out with assumed electron energy of 30 keV. Keeping all other parameters of the setup fixed, the simulations predict that it should be possible to compress up to 600,000 electrons in a $300\ \mu\text{m}$ diameter bunch with sub-300 fs temporal duration.

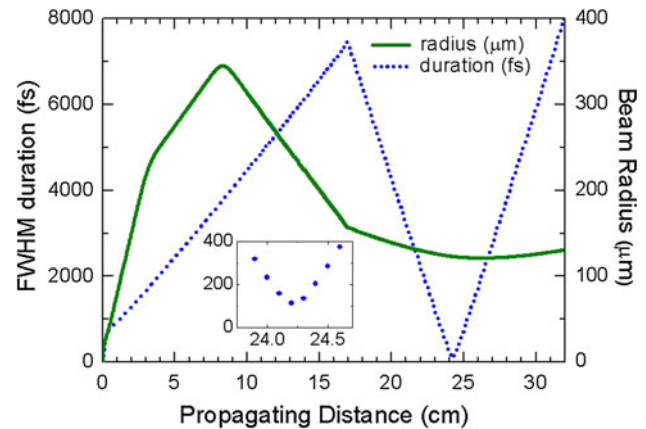


Fig. 4 ASTRA simulation of the evolution of longitudinal and radial bunch dimensions for the present 20 kV electron compressor setup. All distances are as shown indicated in the text, and the assumed electron number is 26,000. The inset is a magnification of the bunch behaviour at the temporal focus, and the simulations predict that a temporal duration of 100 fs should be achievable

3 Results and discussion

First, we determine the shortest possible pulse duration achievable with the compressor, without the constraints of a small spot size at temporal focus, as this provides an estimate of the timing jitter of the device. With the electron number set to about 15,000, the first magnetic lens was adjusted to give reasonable beam collimation at the compressor, but the second magnetic lens was switched off. This allowed the beam size to be large (several mm) at the temporal focus position. After optimisation of the compressor phase, the compressor voltage was increased in steps of about 100 V and streak images were taken at each voltage setting. The results can be seen in Figs. 5 and 6.

Figure 5 displays streak images recorded for applied compressor voltage settings in the 0–2,200 V range. The leftmost frame shows the streak image of the uncompressed pulse (compressor voltage is zero). The subsequent frames show the streak images for increasingly larger compressor voltages. Clearly the pulse duration decreases steadily, culminating in a minimal streak length at 1,800 V, beyond which over-compression occurs that results in an increase in streak length. The temporal durations corresponding to the streak lengths at each voltage value are plotted in Fig. 6. The temporal durations were calculated by a deconvolution procedure involving the streak velocity and unstreaked spot size at the detector [25]. A minimal pulse duration of 200 fs at 1,800 V compressor voltage, together with the established low jitter nature of the streak camera ($<150\ \text{fs}$) [25] experimentally proves that the temporal jitter of the compressor is sub-200 fs, at least over a time span equal to the measurement duration, which was 6 s. However, the applicability of the compressor design in

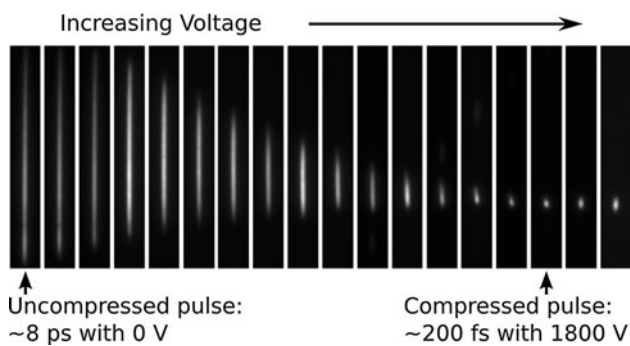


Fig. 5 Streak images on the MCP detector for different voltages on the compressor. The electron number was 15,000 at an electron energy of 20 kV, and the second magnetic lens was switched off, resulting in no collimation at temporal focus (beam radius >1 mm)

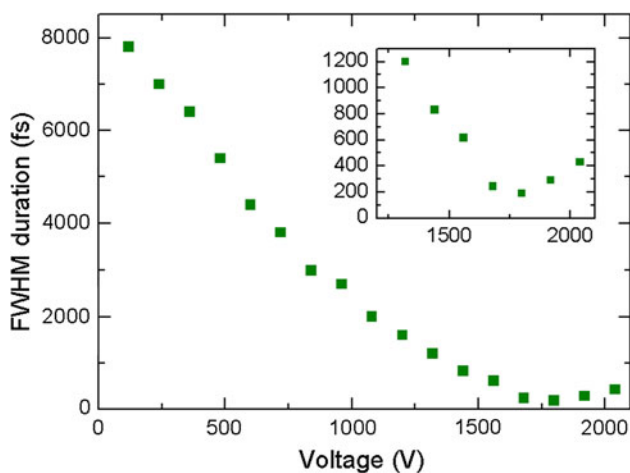


Fig. 6 Pulse duration versus applied compressor voltage for bunches containing 15,000 electrons. For these measurements, the second magnetic lens was switched off so that there was no appreciable radial bunching of the beam at the temporal focus. While such a beam is not useful in diffraction experiments, very short pulse durations down to 200 fs were achieved, demonstrating the low-jitter nature of the compressor

time-resolved electron diffraction experiments crucially depends on its long-term stability. While the established sub-200 fs timing jitter result strictly speaking only extends over a measurement period of a few seconds, it is reasonable to assume that it is also valid for longer times. This is because both the photo cathode laser pulse in the electron gun and the two GaAs PCSS trigger laser pulses are initially split off the same fs laser pulse, which locks them in time to better than 10 fs. The dominant jitter source for GaAs PCSS devices is a variation in trigger laser pulse energy. The CPA2101 is stable within 1 % for more than 24 h, which is equal to the measured average shot to shot intensity variation. In addition, laser beam pointing instabilities, which could also lead to effective trigger intensity variations, are corrected automatically in our

setup by means of piezo-driven mirrors and cameras. Thus, any long-term temporal drift does not contribute to the established 200 fs short-term timing jitter, and in our setup such long-term beam stabilisation was necessary.

Next, the experiment was repeated with a properly shaped and collimated beam, as would be required for an electron diffraction experiment. The results can be seen in Fig. 7. Two different electron numbers, 6,000 and 26,000, were used, and the beam diameter at the streak camera position was 300 μm . Clearly, the minimal pulse durations with a small spot size constraint become somewhat longer (730 and 450 fs at 26,000 and 6,000 electrons, respectively), which is to be expected due to the larger space charge potential opposing compression for this case. Even with a small electron number, however, the pulse duration does not closely approach the ~ 200 fs level observed for the centre of the unfocused bunch. This could be explained by noting that, in the more tightly focused bunch, electrons from a much wider range of radial bunch positions enter the small streak camera aperture. Electrons that have travelled on a wider radial arc through the lens system would thus arrive later than for instance those travelling on the optical axis, resulting in a temporal spread that increases the longitudinal emittance or, equivalently, decreases the compressibility of the pulses. For small electron numbers as the 6,000 electrons/pulse case here, it should also be noted that the bunch expansion pre-compressor is much less than for larger electron numbers. This smaller temporal duration σ_t at injection implies a smaller relative compression energy spread $\Delta E_{k,r}$ to be imparted on the pulse according to Eq. 2 in the appendix. Combined with a presumably large longitudinal emittance, the compression ratio in this case is small as is evident from Fig. 7.

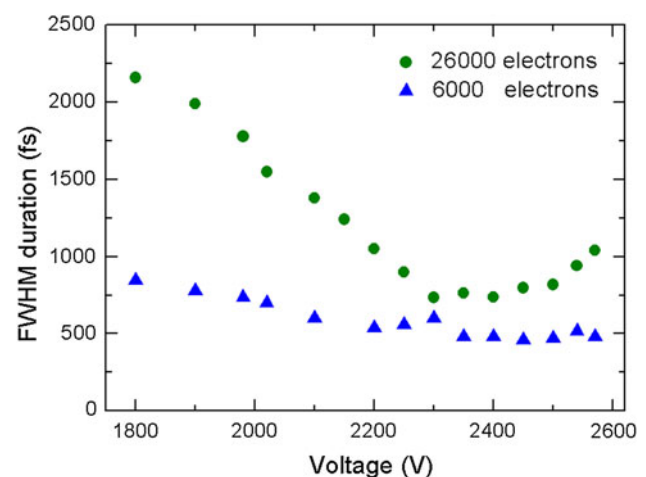


Fig. 7 Pulse duration at temporal focus versus applied compressor voltage for bunches containing 26,000 and 6,000 electrons respectively. The electron bunches are also collimated to a radial beam size of 300 μm . Radial shaping seems to have a negative impact on the achievable pulse duration

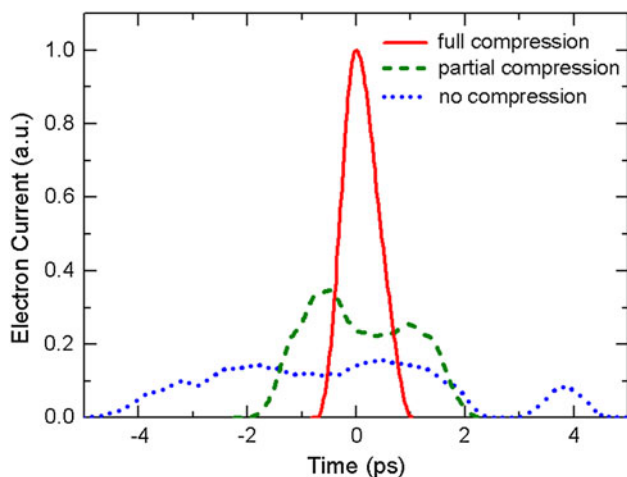


Fig. 8 Extracted electron current profiles for different compressor voltages in case of the 26,000 electron bunches shaped to 300 micron radial diameter. Partial and full compression correspond to compressor voltage settings of 1,800 and 2,300 V respectively

The argument of magnetic lens-induced longitudinal emittance growth does not, however, explain the discrepancy between the experimental results of Figs. 6 and 7 and the simulation shown in Fig. 5, since the pulse durations in the simulation are computed for the entire radial extent of the pulses, and therefore take radial temporal broadening into account. Possibly the beam radii at unmeasured positions in the experiment were larger than in the simulation, increasing this effect. A more important reason is probably unoptimal longitudinal and transverse space charge expansion caused by temporally and spatially inhomogeneous photoemission dynamics at the cathode. The temporal electron current profiles for the 26,000 electrons per pulse case, as shown in Fig. 8, attest to this.

For the optimal case of small pancake-like bunches emitted homogeneously from the photocathode, they would be expected to evolve into a hard edged uniformly populated ellipsoidal shape [27] which, when sampled on a narrow radial region close to the optical axis (as done by the streak camera here), should yield a top-hat temporal distribution. Uniform ellipsoidal pulses are known for their excellent compressibility, while poor compressibility would be expected when there is significant deviation from this ideal shape. The measured uncompressed temporal distribution in Fig. 8 is certainly not top-hat in shape, instead exhibiting a slow-rising double-humped main pulse followed rather curiously by a post-pulse. Partial compression superimposes main and post pulses while enhancing the double-humped feature. While full compression results in a smooth bell-shaped profile, the temporal duration is not as short as simulations would predict, which is not surprising considering the irregular temporal profile of the uncompressed pulse.

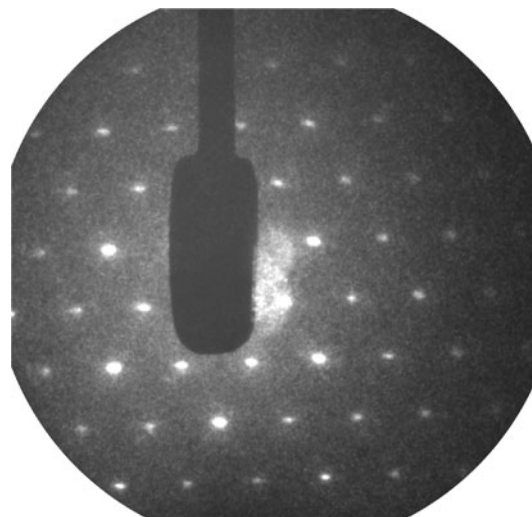


Fig. 9 Diffraction pattern of a free standing TaSe₂ film recorded using compressed electron bunches that contain 26,000 electrons. The image is averaged over 6,000 shots

At the present time, we can only speculate on the cause of the unexpected irregular temporal profiles of our electron pulses. The most likely cause is large inhomogeneities of the photoemission efficiency at the cathode, caused by laser-induced damage and surface contamination.

In order to verify that the compressed electron pulses can in principle be used for electron diffraction experiments, we have placed a sample of a 50 nm thick TaSe₂ crystal of hexagonal symmetry in the beam path at the position of full temporal compression. The resulting diffraction pattern of this charge density wave material is seen in Fig. 9. The image was recorded over 6 s at a repetition rate of 1 kHz. While the Bragg peaks are clearly visible, there appears to be some astigmatism, probably caused by the lack of radial symmetry of the compressor. Changes to the compressor geometry could make the fields surrounding the electron path more homogeneous, thus reducing the astigmatism. One could, for instance, add tube-like metal extrusions around the electron apertures between the compressor plates, providing a smaller but more symmetric electric field gap for the compressor. Thus, while some optimisation is still required, our compressor setup is certainly capable of producing usable diffraction patterns.

The compressor in this work was tested at a relatively low electron energy of 20 keV. Since transmission high energy electron diffraction is typically carried out at higher energies than this, up to the few 100 keV range, it is important to discuss the requirements that would have to be met if this compressor concepts were to be implemented at higher energies. In the appendix, a formula (Eq. 2) is given which estimates the scaling of compressor performance with electron energy. It turns out that the maximum voltage that can be switched by the compressor is the key determining factor for

producing a given relative energy bandwidth $\Delta E_{k,r}$ at a certain electron energy ΔE_k . In the sub-relativistic regime, Eq. 2 shows that the required switched voltage increases roughly proportionally with E_k . The only way to significantly improve the performance of the current compressor concept at higher electron energies is therefore to develop GaAs PCSS's with a higher voltage switching capability. The quality of the switch ohmic contacts in particular must be improved if progress is to be made here.

4 Summary and conclusion

We have introduced a novel experimental method for the temporal compression of chirped expanding electron pulses, which is of particular interest in the context of UED. The heart of the compressor is a few millimeter sized open resonant structure incorporating as low-jitter oscillation trigger a pair of GaAs photoconductive semiconductor switches. Its compactness ensures both a large resonant frequency and consequent high long-term temporal stability of better than 100 fs. It allows to compress electron bunches with a measured jitter of <200 fs, and 26,000 electrons were compressed to 730 fs in a beam diameter of 300 μm . Numerical simulations suggest that its potential capabilities in terms of electron bunch charge and temporal duration greatly exceed the current experimental results. According to these simulations, up to 600,000 electrons could be compressed into a 300 mm diameter sub-300 fs pulse that has sufficiently good coherence for typical UED measurements. In this study, we have argued that the discrepancy between simulation and results can be explained by unoptimal space charge expansion dynamics, which may itself be caused by inhomogeneous photoemission dynamics at the cathode. Use of damage and contamination-free photocathodes, as well as more optimal spatial and temporal shaping of the UV trigger pulse will likely not only result in more highly charged, shorter pulses, but also provide better beam coherence necessary for useful diffraction images.

In conclusion, we believe that our results represent a very promising proof of principle demonstration of an alternative electron bunch compressor suitable for time-resolved diffraction experiments. Its simple and cheap design allows implementation in all non-relativistic UED sources, opening up the applicability of the method to a wide range of sensitive specimens and non-regenerative processes.

Acknowledgments This work is based upon research supported by the South African Research Chair Initiative of the Department of Science and Technology and the National Research Foundation. We

would like to thank Paul Papka for his help with the electron current measurements.

Appendix: A formula for pulsed compressor performance

The compressor described in this paper can be approximated by a parallel plate capacitor with a harmonically ramped axial electric field between the plates separated by distance d , complete with apertures for electron pulses to pass through in the axial direction (see figure and Fig. 6.7 in Ref. 23). Subject to the assumption that the electron pulse transit time through the compressor is less than $T/3$, where T is the oscillation period of the harmonic electric field dependence, the latter can be considered approximately linear. Furthermore, if the electron pulse duration σ_t is much smaller than $T/3$, it can be shown that the rms energy spread ΔE_k that is imparted on an electron pulse of rms pulse duration σ_t , is given by [23]

$$\Delta E_k = \frac{\gamma}{\beta^2 \gamma^2 + 1} v_z \Delta E \sigma_t \quad (1)$$

where γ is the Lorentz factor, $\beta = v_z/c$ with v_z the electron velocity, and ΔE the electric field difference between the time at which the bunch enters and exits the compressor field respectively. Now, assuming a linear electric field ramp dE/dt such that $\Delta E = dE/dt \times d/v_z$, using the fact that the voltage gradient $dV/dt = dE/dt \times d$, and re-writing in terms of the relative rms energy spread $\Delta E_{k,r} = \Delta E_k/E_k$, Eq. 1 yields

$$\Delta E_{k,r} = \frac{\gamma}{\beta^2 \gamma^2 + 1} \frac{\sigma_t}{E_k} \frac{dv}{dt} \quad (2)$$

In the subrelativistic regime, $\gamma/(\beta^2 \gamma^2 + 1)$ varies slowly with energy E_k , and consequently the required compressor voltage to achieve a desired $\Delta E_{k,r}$ at fixed compressor frequency and injected pulse duration scales roughly linearly with E_k .

References

1. M. Eichberger, H. Schäfer, M. Krumova, M. Beyer, J. Demsar, H. Berger, G. Moriena, G. Sciani, R.J.D. Miller, Snapshots of cooperative atomic motions in the optical suppression of charge density waves. *Nature* **468**, 799–802 (2010)
2. E. Möhr-Vorobeva, S. Johnson, P. Beaud, U. Staub, R. De Souza, C. Milne, G. Ingold, J. Demsar, H. Schaefer, A. Titov, Non-thermal melting of a charge density wave in TiSe_2 . *Phys. Rev. Lett.* **117**(036403), 1–4 (2011)
3. M. Woerner, F. Zamponi, Z. Ansari, J. Dreyer, B. Freyer, M. Prémont-Schwarz, T. Elsaesser, Concerted electron and proton transfer in ionic crystals mapped by femtosecond X-ray powder diffraction. *J. Chem. Phys.* **133**, 064509 (2010)

4. K. Sokolowski-Tinten, C. Blome, J. Blums, A. Cavalleri, C. Dietrich, A. Tarasevitch, I. Uschmann, E. Förster, M. Kammler, M. Horn- von Hoegen, D. von der Linde, Femtosecond X-ray measurement of coherent lattice vibrations near the Lindemann stability limit. *Nature* **422**, 287–289 (2003)
5. A. Morak, T. Kämpfer, I. Uschmann, A. Lübcke, E. Förster, R. Sauerbrey, Acoustic phonons in InSb probed by time-resolved X-ray diffraction. *Phys. Status Solidi B* **12**, 2728–2744 (2006)
6. C. Reich, P. Gibbon, I.E.F. Uschmann Yield optimization and time structure of femtosecond laser plasma K α sources, *Phys. Rev. Lett.* **84**, 4846–4849 (2000)
7. M. Hagedorn, J. Kutzner, G. Tsimilis, H. Zacharias, High-repetition-rate hard X-ray generation with sub-millijoule femtosecond laser pulses. *Appl. Phys. B* **77**, 49–57 (2003)
8. www.desy.de/~mpyflo/. Accessed 1 Apr 2012
9. B.J. Siwick, R.J.D. Miller, Femtosecond electron diffraction studies of strongly driven structural phase transitions. *Chem. Phys.* **299**, 285 (2004)
10. C.T. Hebeisen, G. Sciaini, M. Harb, R. Ernstorfer, T. Dartigalongue, S.G. Kruglik, R.J.D. Miller, Grating enhanced ponderomotive scattering for visualization and full characterization of femtosecond electron pulses. *Opt. Express* **16**, 3335 (2008)
11. B. Siwick, J. Dwyer, R. Jordan, D. Miller, An atomic view of melting using femtosecond electron diffraction. *Science* **302**, 1382–1385 (2003)
12. H. Park, X. Wang, S. Nie, R. Clinite, J. Cao, Direct and real-time probing of both coherent and thermal lattice motions. *Solid State Commun.* **136**(9–10), 559–563 (2005)
13. P. Baum, D.-S. Yang, A. Zewail, 4D visualization of transitional structures in phase transformations by electron diffraction. *Science* **318**, 788–792 (2007)
14. P. Musumeci, J.T. Moody, C.M. Scoby, M.S. Gutierrez, H.A. Bender, N.S. Wilcox, High quality single shot diffraction patterns using ultrashort mega-electronvolt electron beams from a radio frequency photoinjector. *Rev. Sci. Instrum.* **81**, 013306 (2010)
15. B.J. Siwick, J.R. Dwyer, R.E. Jordan, R.J.D. Miller, Ultrafast electron optics: propagation dynamics of femtosecond electron packets. *J. Appl. Phys.* **92**, 1643 (2002)
16. T. van Oudheusden, E.F. de Jong, S.B. van der Geer, W.P.E.M. Root, O.J. Luiten, B.J. Siwick, Electron source concept for single-shot sub-100 fs electron diffraction in the 100 keV range. *J. Appl. Phys.* **102**(9), 093501 (2007)
17. E. Fill, L. Veisz, A. Apolonski, F. Krausz, Sub-fs electron pulses for ultrafast electron diffraction. *New J. Phys.* **8**, 272 (2006)
18. T. van Oudheusden, P.L.E.M. Pasmans, S.B. van der Geer, M.J. de Loos, M.J. van der Wiel, O.J. Luiten, Compression of sub-relativistic space-charge-dominated electron bunches for single-shot femtosecond electron diffraction. *Phys. Rev. Lett.* **105**(26), 264801 (2010)
19. G. Kassier, K. Haupt, N. Erasmus, E. Rohwer, H. Schwoerer, Achromatic reflectron compressor design for bright pulses in femtosecond electron diffraction. *J. Appl. Phys.* **105**, 113111 (2009)
20. Y. Wang, N. Gedik Electron pulse compression with a practical reflectron design for ultrafast electron diffraction, *IEEE J. Sel. Topics Quantum Electron.* (2011)
21. S. Tokita, M. Hashida, S. Inoue, T. Nishoji, K. Otani, S. Sakabe, Single-shot femtosecond electron diffraction with laser-accelerated electrons: experimental demonstration of electron pulse compression. *Phys. Rev. Lett.* **105**, 215004 (2010)
22. J. Faure, C. Rechatin, A. Norlin, A. Lifschitz, Y. Glinec, V. Malka, Controlled injection and acceleration of electrons in plasma wakefields by colliding laser pulses. *Nature* **444**, 737–739 (2006)
23. G. H. Kassier Ultrafast electron diffraction: source development, diffractometer design and pulse characterisation. PhD Thesis, Chapter 6, University of Stellenbosch, Stellenbosch (2010)
24. A. Janzen, B. Krenzer, O. Heinz, P. Zhou, D. Thien, A. Hanisch, F. Heringdorf, D. von der Linde, M. von Horn Hoegen, A pulsed electron gun for ultrafast electron diffraction at surfaces. *Rev. Sci. Instrum.* **78**, 13906 (2007)
25. G. Kassier, K. Haupt, N. Erasmus, E. Rohwer, H. von Bergmann, H. Schwoerer, S. Coelho, D. Auret, A compact streak camera for 150 fs time resolved measurement of bright pulses in ultrafast electron diffraction. *Rev. Sci. Instrum.* **81**(105103), 1–5 (2010)
26. <http://laacg1.lanl.gov/laacg/>. Accessed 1 Apr 2012
27. O.J. Luiten, S.B. van der Geer, M.J. de Loos, F.B. Kiewiet, M.J. van der Wiel, *Phys. Rev. Lett.* **93**, 94802 (2004)